Thermal Chemical Energy Storage

May 2020

by

Mechanical, Aerospace and Biomedical Engineering (MABE)
Undergraduate Students

Authors

James McBroom
Samuel Swayne
Jonathan West
John Davis
Tennessee Bryant

and

MABE Advisor Dr. William (Bill) Miller

**University of Tennessee, College of Engineering,
Mechanical, Aerospace and Biomedical Engineering**

for the

**UTK Office of Sustainability
2233 Volunteer Boulevard, R, 208C
Knoxville, Tennessee 37996**

CONTENTS

Page

LIST OF FIGURES iii
LIST OF TABLES iv
ACRONYMS v
1. INTRODUCTION 1
2. THERMAL CHEMICAL ENERGY STORAGE 2
2.1 ENERGY STORAGE COMPOUNDS 2
2.1.1 Potassium Nitrate (KNO_3) 2
2.1.2 Lithium Hydroxide (LiOH) 2
2.1.3 Sodium Hydroxide (NaOH) 3
2.2 PHYSICAL MODELING 3
2.2.1 Test Stand 3
2.3 EXCEL MODELING 4
2.3.1 Excel Parabolic Solar Collector (PSC) Temperature Model 4
2.3.2 Excel Model Results 5
2.4 ENERGYPLUS SIMULATIONS 8
2.4.1 Overview 8
2.4.2 Data Reduction 9
2.4.3 Simulation Results 9
3. CONCLUSIONS 11
4. REFERENCES 12

LIST OF FIGURES

Figure **Page**

Figure 1: Test Stand Apparatus 3
Figure 2: Tube Cross Section Temperatures 4
Figure 3: Cost on a Monthly Basis 9

LIST OF TABLES

Table **Page**

Table 1: Temperatures (°C) and heat transfer rates (W) at exit of the PSC tube 6
Table 2: Syltherm exit temperatures for various flow rates 6
Table 3: Exit temperatures for different tube lengths 7
Table 4: Temperatures (°C) and heat transfer rates (W) for different irradiances 8
Table 5: Average global horizontal irradiance 8
Table 6: Large Hospital Heating Costs 9
Table 7: Secondary School Heating Costs 9
Table 8: Large Hotel Heating Costs 10
Table 9: Large Office Building Heating Costs 10

ACRONYMS

PSC	Parabolic Solar Collector
TCES	Thermal Chemical Energy Storage
VB	Visual Basic

INTRODUCTION

The Tennessee Valley Authority (TVA) and one of its many distributors, the Knoxville Utility Board, provide all electrical service to the University of Tennessee (UTK) campus. UTK generates steam at its boiler plant for comfort conditioning of its buildings in the winter. UTK uses a water chilling system for comfort cooling and has 5 chiller plants at various locations on campus. Each plant is equipped with about 5,000 tons of refrigerant capacity for chilling water or brine that is pumped to buildings on campus for comfort cooling through use of terminal units or fan-coil type units. (Note: A refrigerant ton is equivalent to 12,000 Btu per hour of cooling, which in an 8-hour day produces one ton of ice.)

The University has an ambitious long-term plan for new building construction and for the renovation of its existing buildings, all of which will require expansion of the chilled water and steam distribution systems. Therefore, UTK's plans must include the addition of supplementary capacity. Thermal storage has the potential to provide added cooling capacity at less investment than additional chillers. Instead of expanding one of the 5 UTK chiller plants, a chilled water storage or phase change material storage system can be implemented adjacent to existing buildings or underneath in the basement of new buildings. The storage can then serve the cooling load of the building by day and be regenerated the following night with the existing central chillers, operating on off peak power. The storage system will cost less than the new chiller. For the case where the existing chiller is operating at its full capacity, the thermal storage can save lots of money. As an example, the United States Army Corp of Engineers (USACE) and the Construction Engineering Research Laboratory (CERL) designed and showcased at Fort Jackson, SC a large capacity (2.25M gal) chilled water cooling system for their Central Plant No. 2. The system operates successfully and was monitored for a 5-year period, resulting in an annual electrical utility cost savings of $0.43M. Thermal performance exceeded the design goal of shifting 3,000 kW of on-peak demand to off-peak periods. Therefore, it has been demonstrated that thermal storage is an effective system for utility load shifting and can provide adequate energy savings to justify its use.

THERMAL CHEMICAL ENERGY STORAGE

The objective of Thermal Chemical Energy Storage (TCES) is to convert heat energy to chemical energy for later use. This project used sodium hydroxide (NaOH) with a Parabolic Solar Collector (PSC). The PSC captured heat from solar radiation. The collected heat could be used to decompose the NaOH solution, effectively storing heat in chemical bonds. Physical tests and computer models determined the PSC's ability to raise the coolant fluid to a suitable temperature for NaOH decomposition. EnergyPlus simulations were used to determine the potential cost savings for buildings in various cities.

ENERGY STORAGE COMPOUNDS

Various compounds were investigated to determine energy storage suitability. The property of concern was the endothermic reaction's activation (charging) temperature. This indicates the working fluid's required temperature to store energy in the chemical bonds. The energy density was also studied to determine energy storage efficiency. The investigated compounds were KNO_3, LiOH, and NaOH.

Potassium Nitrate (KNO_3)

Potassium Nitrate (KNO_3) can be created from a double replacement reaction. An example of a double displacement reaction is KCl reacting with $NaNO_3$ to create KNO_3 and NaCl. Creating KNO_3 would be easier than acquiring it.

KNO_3 has an energy storage capacity of 117 kJ/kg. The activation temperature is 337 °C. The energy storage capacity is low relative to other compounds. The activation temperature is very high, especially for an energy storage system that is not designed to reach high temperatures. [1] [2]

Given its low energy storage capacity and high activation temperature, KNO_3 is unsuitable for the project.

Lithium Hydroxide (LiOH)

Lithium hydroxide (LiOH) is commonly found as the monohydrate LiOH·H2O due to its hygroscopic nature. It can be formed by elemental lithium reacting with water. Alternatively, it can be formed from lithium oxide, a reaction which releases a large amount of energy. However, the reverse reaction requires an activation temperature between 400-500 °C. This is undesirable for low temperature energy storage applications such as this one. Additionally, LiOH is very corrosive, hazardous, and dangerous to store. Glass or porcelain can also corrode from LiOH. [3]

Another considered reaction was the hydration of LiOH. Since this is a hygroscopic crystal, heating it can release water molecules from the hydrate. The recombination of LiOH and H_2O is exothermic. This does not yield as much heat as the sodium hydroxide (NaOH) reaction. The storage process requires a lower activation temperature and could store energy effectively. However, it would require a larger volume to store the same amount of energy when compared to using NaOH. Corrosiveness is still an issue for storage, even when using the hydration reaction. The required activation temperature for LiOH dehydration is 64 °C. The energy storage capacity is 1440 kJ/kg (950 MJ/m^3), which is less than some chemical energy storage options but of similar magnitude. This dehydration reaction would have required a vacuum and specially formed carbon structures to reach an adequate reaction rate. [3]

Because of its drawbacks, LiOH was classified as an unsuitable candidate compared to NaOH, which was previously used in this project.

Sodium Hydroxide (NaOH)

Sodium hydroxide (NaOH) is commonly found as a white solid ionic compound. NaOH was chosen because of its advantages over the other chemicals. NaOH has an energy storage capacity of 900 MJ/m^3, which is slightly lower than LiOH's energy storage capacity. NaOH has an activation temperature of 300 °C, which is greater than the LiOH dehydration temperature but lower than the activation temperature of KNO_3. [4] NaOH is also cheap and readily available, so the chemical can be easily acquired. NaOH was also previously used in this project with success. As a result, sodium hydroxide was the chosen chemical for energy storage in this application.

PHYSICAL MODELING

Test Stand

A physical testing apparatus was assembled to conduct tests on the Parabolic Solar Collector (PSC). The test stand was a pre-existing apparatus built by a previous design team. The test stand primarily consisted of glassware and plastic tubes. The PSC used in this test stand consisted of two concentric glass tubes separated by a vacuum. The PSC was mounted above a parabolically shaped metal sheet.

Teflon plastic tubes were used for the fluid inlet and exit of the collector. A glassware reactor vessel and heat exchanger were used for the NaOH reaction. Water was used as the working fluid in initial tests. Industrial work lights were used as the light source. Using this setup, the water temperature increased from 25 °C to 40 °C after approximately one hour. A rotameter controlled the fluid flow rate. An improved gravity-fed pump-priming mechanism was added to make test startup simpler. The test stand is shown in the figure below.

Figure 1: Test Stand Apparatus

It was proposed that other fluid types, such as a mineral oil or synthetic heat transfer fluid, could reach higher exit temperatures. The Dow chemical Syltherm XLT was chosen as the working fluid. Syltherm was chosen because of its properties and temperature range.

Unfortunately, no more tests were conducted due to the COVID-19 lockdown. The PSC was numerically modeled in Excel to determine the system's potential for thermal chemical energy storage.

EXCEL MODELING

Excel Parabolic Solar Collector (PSC) Temperature Model

Microsoft Excel's Visual Basic (VB) editor feature modeled the PSC temperatures. This tool was previously created for earlier testing of the prototype. However, convergence was never achieved for all tube segments. The model's primary goal was to determine the collector's capability to heat oil for dissociating sodium hydroxide.

The program accepted various user inputs highlighted in blue. Examples of user inputs were tube diameter, tube length, assumed solar irradiance, flow rate, and inlet temperature. Heat transfer energy balance equations were derived for two concentric tubes with an annular vacuum region. Temperatures and heat transfer rates were calculated for each tube surface and the inner fluid. Unlike the test stand with glass tubes in the PSC, the computer model used an inner copper tube and an outer glass tube to increase the energy absorption. Simulations determined this would be a better design due to the increased conductivity through the inner tube's wall. Calculations were done iteratively using a Gauss-Seidel numerical approach with a relaxation of 0.001. These iterations were also done on small segments of the total tube length to account for any potential nonlinearity in the temperatures. These segments were set to 0.25 meters in length for most of the simulations. The primary tube length tested was 10 meters.

The program reported five temperatures for each segment after achieving convergence. The fluid entrance temperature for the segment, $T_{ci,}$ was also reported. The same five temperatures were also recorded at the tube's outlet. These five temperatures (T_1, T_2, T_3, T_4, T_5) consisted of the four wall temperatures and the fluid temperature according to the diagram below. The heat transfer rates, including both short-wave and long-wave radiation, were also calculated at each point and reported for the final segment.

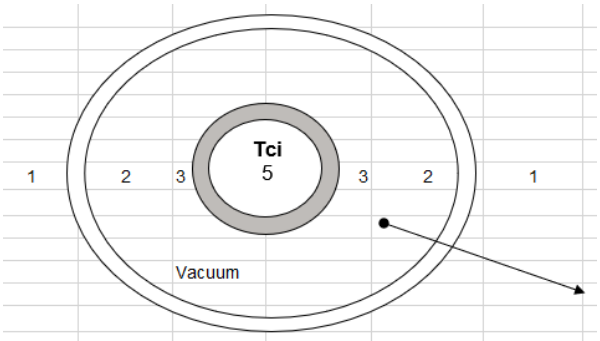

Figure 2: Tube Cross Section Temperatures

A convergence issue was initially occurring between segments 16 – 21, or from 4.00 m – 5.25 m. Relaxing the convergence criteria reduced the iterations. This relaxation helped with the divergence issue for one or two segments. However, upon further investigation, it was determined that the problem was not a coding error as much as a mathematical error. The effective radiation heat transfer coefficient was negatively diverging for certain tube segments. This divergence was a result of a fourth-power temperature difference in the equation. This divergence was resolved by a time linearization of the equation, which eliminated the difference term and relied solely on additive terms. This correction also prevented negative heat transfer coefficients from emerging.

Other mathematical issues were identified and subsequently corrected. The outer tube surfaces' heat transfer rate equation (q_1 and q_2) did not include the solar irradiance. Also, the view factor between the outer and inner tubes was not properly accounted for when calculating the solar energy absorbed by the outer tube. Both issues affected the temperature calculations.

The program ran smoother after making the corrections. Acceptable temperature values were obtained for all tube segments with full convergence. Run time was still significantly reduced by the looser convergence criteria. This improvement was kept even after correcting mathematical errors.

The initial program was modeled with water as the internal fluid. However, a synthetic heat transfer fluid was tested as well. Properties for the Dow chemical Syltherm XLT were obtained from the company's publication. The properties were added to the model to compare the heating effectiveness of Syltherm and water. However, only six temperature-dependent data points were available for each necessary property (density, dynamic viscosity, specific heat, and thermal conductivity). Regression curves were generated from the properties. Matlab's *polyfit()* function obtained curve fit equations to be used in the Visual Basic code. The viscosity was the most difficult property to fit with a polynomial. The data showed exponential behavior, but an exponential model did not fit well. Thus, a fourth-order polynomial was used.

Syltherm was tested as the primary heat transfer fluid. The tests yielded a significantly higher exit temperature. This confirmed that Syltherm would be more effective than water for reaching higher temperatures to activate the NaOH decomposition.

An important note should be made concerning curve fitting. According to the Dow Technical Data Sheet, Syltherm XLT's recommended temperature range is -100 °C to 260 °C. Because of this, the polynomial fit should not be used much beyond this range. The freezing point of the Syltherm is -111 °C. The estimated critical temperature is 327 °C [5]. Therefore, operation outside of the recommended range would not be advisable. The data points used for the polynomial fit ranged from -100 °C to 280 °C. Therefore, the curve cannot be considered valid outside of this range. When testing large tube lengths, the model crashed because the exit temperature exceeded this value. To resolve the problem, all Syltherm XLT property data was computed for a temperature of 276.8 °C (550 K) if the temperature leaving the collector exceeded this value. Alternatively, other heat transfer fluids suitable for higher temperature ranges could be included in the code.

Excel Model Results

Various conditions were tested for refining the model. Two parameters tested were the type of working fluid and the fluid entrance temperatures. Different flow rates, tube lengths, and solar irradiance values were also tested to determine the effect on exit temperature. Wind speed was set at 0.5 m/s. The outer glass tube used in the model computations had an external and internal diameter of 50 mm and 40 mm, respectively. The inner copper tube was modeled with an external and internal diameter of 36 mm and 32 mm, respectively. The inner tube outside diameter was increased over previous versions to maximize the view factor between the two surfaces and allow more heat transfer. All values were calculated in 0.25 m tube segments. The results of these trials are detailed in the sections below.

Heat Transfer Fluid & Inlet Temperature

The inlet temperature of 21 °C was tested since this is approximately room temperature. However, because the heat transfer fluid is recirculated and the system is at steady state, it is reasonable to assume the heat transfer fluid would enter the absorber tube at a higher temperature than on initial startup. Thus, 31 °C was also tested for both fluids to determine the effect on performance. Since the Syltherm heat transfer fluid yielded the best temperature results, an additional test was performed for this fluid with a higher entrance temperature of 41 °C. The inlet temperature tests were conducted with an assumed constant solar irradiance of 300 W/m^2 and a flow rate of 1.0 GPM. The length was set to 10 m with 0.25 m segments.

Table 1: Temperatures (°C) and heat transfer rates (W) at exit of the PSC tube

	Water		Syltherm		
	T_{ci} = 21 °C	T_{ci} = 31 °C	T_{ci} = 21 °C	T_{ci} = 31 °C	T_{ci} = 41 °C
T_1	103.98 °C	104.20 °C	59.36 °C	59.46 °C	59.59 °C
T_2	118.26 °C	118.47 °C	73.49 °C	73.59 °C	73.70 °C
T_3	41.13 °C	50.22 °C	97.00 °C	104.26 °C	112.17 °C
T_4	41.12 °C	50.21 °C	96.99 °C	104.25 °C	112.17 °C
T_5	34.13 °C	44.07 °C	58.13 °C	68.11 °C	78.10 °C
Q_1	-108.45 W	-109.70 W	-107.94 W	-107.78 W	-107.60 W
Q_2	-97.98 W	-98.15 W	-97.28 W	-97.20 W	-97.11 W
Q_3	-97.98 W	-98.15 W	-97.28 W	-97.20 W	-97.11 W
Q_4	-87.73 W	-88.40 W	-87.52 W	-87.45 W	-87.36 W
Q_5	-81.88 W	-85.11 W	-87.24 W	-87.23 W	-87.19 W

For water with an entrance temperature T_{ci} = 21°C in a 10 m tube, the temperature change was 13.13°C with an exit temperature of 34.13°C. Using Syltherm as the heat transfer fluid increased the temperature difference to 37.13°C with a final exit temperature of 58.13°C. Furthermore, increasing the entrance temperature to 31 °C with the Syltherm allowed the exit temperature to reach 68.11 °C. A 41 °C entrance temperature caused the exit temperature to reach 78.10 °C. This approaches sodium hydroxide's necessary charging temperature. The heat transfer rates were calculated with the convention of outward heat transfer (away from the working fluid) as positive. Thus, all heat transfer values listed in the table are negative. The simulations determined that Syltherm would be a better choice for coolant in the PSC because it could reach higher temperatures with the same tube length and energy input.

Flow Rate

The Excel simulation was also tested for Syltherm flow rate conditions at an inlet temperature of 35 °C and a tube length of 10 m. The solar irradiance used for these tests was 300 W/m^2. This data is displayed in Table 2.

Table 2: Syltherm exit temperatures for various flow rates

Flow Rate	Exit Temperature (T_5)
1.0 GPM	72.27 °C
1.2 GPM	66.05 °C
2.0 GPM	53.62 °C
3.0 GPM	47.42 °C
4.0 GPM	44.32 °C
5.0 GPM	42.46 °C

The data demonstrates that a slower flow rate will contribute to a higher exit temperature. Thus, a slower flow rate would be better to reach temperatures for dissociating NaOH. However, a lower flow rate could decrease the heat transfer rate from the working fluid to the NaOH solution. This would have to be considered when determining ideal flow rate.

Tube Length

The Excel model was run with various tube lengths to determine the required tube length for desired exit temperatures. Tests were run with a solar irradiance of 300 W/m^2 and an inlet fluid temperature of 31 °C. The test results are displayed below in Table 3.

Table 3: Exit temperatures for different tube lengths

Tube Length	Exit Temperature (T_5)
10 m	68.31 °C
20 m	105.69 °C
30 m	143.27 °C
40 m	181.10 °C
50 m	219.25 °C
60 m	257.85 °C
70 m	296.41 °C

Each 10 m increase in tube length corresponded to a nearly 40 °C exit temperature change. From this, a linear relationship can be inferred between tube length and fluid exit temperature. This corresponds to the case of constant heat flux through the tube wall. Ideally, temperatures above 300 °C would be desired for easily dissociating NaOH. However, energy storage could likely be achieved at lower temperatures. A tube length of greater than 70 m would be required to reach these high temperatures, and this would approach the critical temperature of the Syltherm working fluid. Thus, no tests were conducted beyond this length. A heat transfer fluid with a higher working temperature range would be needed for these high temperature applications. However, according to the data above, a moderately-sized collector with a 20 m length could achieve temperatures above 100 °C, which should be sufficient for energy storage.

Solar Irradiance

Tests were conducted to determine the dependence of the PSC performance on global horizontal solar irradiance. For these simulations, the solar irradiance was varied from 100 to 800 W/m^2 in increments of 100 W/m^2. As expected, when the irradiance was increased, the heat transfer and temperatures throughout the solar collector's surfaces also increased. The flow rate for these tests was kept at 1.0 GPM. The fluid inlet temperature was 31 °C. The tube length was 10 m. The temperatures and heat transfer values for various irradiances are recorded in Table 4.

Table 4: Temperatures (°C) and heat transfer rates (W) for different irradiances

	100 W/m^2	200 W/m^2	300 W/m^2	400 W/m^2	500 W/m^2	600 W/m^2	700 W/m^2	800 W/m^2
T_1	59.88 °C	83.56 °C	105.93 °C	126.94 °C	146.95 °C	166.11 °C	184.5 °C	202.29 °C
T_2	64.62 °C	93.03 °C	120.13 °C	145.88 °C	170.63 °C	194.53 °C	217.7 °C	240.18 °C
T_3	54.61 °C	79.10 °C	104.59 °C	124.88 °C	145.74 °C	167.61 °C	190.5 °C	213.90 °C
T_4	54.61 °C	79.09 °C	104.58 °C	124.87 °C	145.72 °C	167.59 °C	190.5 °C	213.88 °C
T_5	43.20 °C	55.86 °C	68.31 °C	80.84 °C	93.46 °C	106.19 °C	119.0 °C	132.01 °C
Q_1	-36.29 W	-72.53 W	-108.75 W	-145.10 W	-181.45 W	-217.79 W	-254.1 W	-290.36 W
Q_2	-32.58 W	-65.13 W	-97.68 W	-130.30 W	-162.91 W	-195.52 W	-228.1 W	-260.68 W
Q_3	-32.58 W	-65.13 W	-97.68 W	-130.30 W	-162.91 W	-195.52 W	-228.1 W	-260.68 W
Q_4	-29.33 W	-58.63 W	-87.93 W	-117.29 W	-146.66 W	-176.02 W	-205.4 W	-234.67 W
Q_5	-29.34 W	-58.66 W	-87.73 W	-117.13 W	-146.57 W	-175.99 W	-205.4 W	-234.68 W

A range of solar irradiance values was chosen instead of testing specific values. This is because solar irradiance varies greatly with city location, time of year, cloud coverage, pollution, and other situational factors. The range for solar irradiance testing was chosen so that it contained the average annual solar irradiance for each of the locations tested by the weather models. The average solar irradiance values were calculated from daily average incident energy as reported by Solar Energy Local and are shown in the table below [6]:

Table 5: Average global horizontal irradiance

City	Irradiance
Atlanta, GA	561.8 W/m^2
Buffalo, NY	459.3 W/m^2
El Paso, TX	731.5 W/m^2
Great Falls, MT	490.3 W/m^2
Tampa, FL	630.3 W/m^2

ENERGYPLUS SIMULATIONS

Overview

EnergyPlus is an open source building-modeling software. EnergyPlus was used to determine potential cost savings for different buildings located in different climates. Simulations were run for the following cities: Atlanta, Buffalo, El Paso, Great Falls, and Tampa. All building files were obtained from the US Department of Energy's Building Energy Codes Program [7]. Typical Meteorological Year (TMY3) weather files were obtained from the EnergyPlus website [8]. All weather files corresponded to the climates in the listed cities' airports. The following building models were analyzed: Large Hospital, Secondary School, Large Hotel, and Large Office. Unfortunately, some of the EnergyPlus files were not updated correctly to the current version of EnergyPlus and would not run. Therefore, some of the building models' results have fewer than five cities.

Data Reduction

It was desired to calculate the cost for using natural gas to heat each building. Each EnergyPlus simulation generated spreadsheets with Output Summary Tables. The data from the Output Summary Tables was called "HEATING:GAS [J]" from the Summary Report "BUILDING ENERGY PERFORMANCE - NATURAL GAS." Data was presented monthly. Dimensional analysis was used to convert the energy consumption (J) to cost ($). Natural Gas Costs in $/1000 ft^3 were obtained from the US Energy Information Administration for the year 2018 [9]. Costs varied for different states. The natural gas cost in a state in $/1000 ft^3 is represented as NG in the below equation since it varied depending on the state.

$$Cost\ (\$) = HEATING{:}\,GAS[J]\,x\ 2.77 * 10^{-7} \left(\frac{kWh}{J}\right) x\ 0.341 \frac{therm}{kWh}\ x \frac{100}{1.036} \frac{ft^3}{therm}\ x \frac{NG}{1000} \frac{\$}{ft^3}$$

Figure 3: Cost on a Monthly Basis

Simulation Results

The monthly calculated costs were added up to determine the yearly costs. The monthly energy consumptions were added up to determine the annual energy consumption. This information is displayed in the below tables. January's energy consumption and monthly costs are also displayed in the below tables. On average from the data, January uses 25% of the annual energy consumption. Peak heating demand occurs in January. Thermal chemical energy storage could offset the peak demand by using stored energy to heat a building. The results of the simulations are summarized in the following tables according to the type of building and geographic location.

Table 6: Large Hospital Heating Costs

City	Annual Cost	Monthly Cost of January	January Cost Percent of Total	Annual Energy (J)	Energy for January (J)
Atlanta, GA	$424,814.98	$52,142.82	12.27 %	5.70×10^{12}	7.00×10^{11}
Great Falls, MT	$422,436.24	$68,434.82	16.20 %	6.53×10^{12}	1.06×10^{12}
El Paso, TX	$245,194.68	$27,303.61	11.14 %	4.11×10^{12}	4.57×10^{11}

Table 7: Secondary School Heating Costs

City	Annual Cost	Monthly Cost of January	January Cost Percent of Total	Annual Energy (J)	Energy for January (J)
Atlanta, GA	$41,350.52	$13,430.65	32.48 %	5.55×10^{11}	1.80×10^{11}
Buffalo, NY	$74,486.09	$18,386.66	24.68 %	1.11×10^{12}	2.74×10^{11}
El Paso, TX	$34,921.66	$8,420.44	24.11 %	5.85×10^{11}	1.41×10^{11}
Great Falls, MT	$91,389.35	$34,708.11	37.98 %	1.41×10^{12}	5.37×10^{11}
Tampa, FL	$16,593.62	$4,285.72	25.83 %	1.62×10^{11}	4.20×10^{10}

Table 8: Large Hotel Heating Costs

City	Annual Cost ($)	Monthly Cost of January ($)	January Cost Percent of Total (%)	Annual Energy (J)	Energy for January (J)
Atlanta, GA	$84,592.98	$21,016.01	24.84 %	1.14×10^{12}	2.82×10^{11}
Buffalo, NY	$107,749.33	$20,669.55	19.18 %	1.61×10^{12}	3.08×10^{11}
El Paso, TX	$35,432.56	$6,686.67	18.87 %	5.93×10^{11}	1.12×10^{11}
Great Falls, MT	$131,148.46	$39,356.13	30.01 %	2.03×10^{12}	6.09×10^{11}
Tampa, FL	$44,202.69	$9,521.61	21.54 %	4.33×10^{11}	9.32×10^{10}

Table 9: Large Office Building Heating Costs

City	Annual Cost	Monthly Cost of January	January Cost Percent of Total	Annual Energy (J)	Energy for January (J)
Buffalo, NY	$212,334.40	$59,777.91	28.15 %	3.16×10^{12}	8.91×10^{11}
El Paso, TX	$19,666.18	$5,257.11	26.73 %	3.29×10^{11}	8.80×10^{10}
Great Falls, MT	$203,505.18	$67,837.52	33.33 %	3.15×10^{12}	1.05×10^{12}
Tampa, FL	$10,157.93	$3,407.85	33.55 %	9.95×10^{10}	3.34×10^{10}

CONCLUSIONS

The Excel simulations gave a reasonable assessment this PSC-based TCES system. From the different variables tested, it was determined that Syltherm XLT or a heat transfer fluid of similar properties would be preferable to water to achieve required temperatures. Additionally, the desired tube length and flow rates can be determined from the model's data. The PSC's performance can also be evaluated based on geographic location and weather patterns based on the solar irradiance data. The collector will be more effective in warmer climates. Colder climates will need this type of energy storage system more. Potentially, moderate climates could be the best location for implementing this system. Furthermore, these areas are more likely to rely on electricity generation for heating sources.

TCES should ideally be used during peak demand. This typically occurs in January when it is cold. With TCES, less energy will be used to heat buildings and therefore fewer costs will be incurred. EnergyPlus simulations found that on average January uses 25% of annual energy consumption. As mentioned above, TCES could be very useful to save costs in colder climates, such as Great Falls and Buffalo. Great Falls and Buffalo both yielded very high energy consumption and heating costs. However, it should be noted that much of the heating in these locations comes from natural gas, while TCES is most beneficial in mitigating peak electrical demand. Note also that the simulations were for individual buildings. Therefore, the consumption, costs, and potential savings would be even greater if implemented across multiple hospitals, offices, schools, and hotels in a city.

REFERENCES

1. Gomez, J., Calvet, N., Starace, A., and Glatzmaier, G., 2013, "Ca(NO3)2—NaNO3—KNO3 Molten Salt Mixtures for Direct Thermal Energy Storage Systems in Parabolic Trough Plants", Journal of Solar Energy Engineering, 135(2).
2. Y. Zhao, R. Wang, L. Wang and N. Yu, "Development of highly conductive KNO3/NaNO3 composite for TES (thermal energy storage)", *Energy*, vol. 70, pp. 272-277, 2014. Available: 10.1016/j.energy.2014.03.127.
3. Li, J., Zeng, T., Kobayashi, N., Xu, H., Bai, Y., Deng, L., He, Z., and Huang, H., 2019, "Lithium Hydroxide Reaction for Low Temperature Chemical Heat Storage: Hydration and Dehydration Reaction", Energies, 12(19), p. 3741.
4. Weber, R., and Dorer, V., 2008, "Long-term heat storage with NaOH", Vacuum, 82(7), pp. 708-716.
5. The Dow Chemical Company. "Syltherm XLT." Technical Data Sheet. n.d.
6. 2020, "Solar Energy & Solar Power in the U.S.", Solar Energy Local [Online]. Available: https://www.solarenergylocal.com/. [Accessed: 03- May- 2020].
7. 2020, "Commercial Prototype Building Models | Building Energy Codes Program", Energycodes.gov [Online]. Available: https://www.energycodes.gov/development/commercial/prototype_models. [Accessed: 03- May- 2020].
8. 2020, "Weather Data by Region | EnergyPlus", Energyplus.net [Online]. Available: https://energyplus.net/weather-region/north_and_central_america_wmo_region_4. [Accessed: 03- May- 2020].
9. "Average Commercial Price – Natural Gas Prices", *Eia.gov*, 2020.